Oriented Binding of the His_6-Tagged Carboxyl-Tail of the L-type Ca^{2+} Channel α_1-Subunit to a New NTA-Functionalized Self-Assembled Monolayer

Roland Gamsjaeger,[†] Barbara Wimmer,[†] Heike Kahr,[†] Ali Tinazli,[‡] Srdjan Picuric,[‡] Suman Lata,[‡] Robert Tampé,[‡] Yves Maulet,[§] Hermann J. Gruber,[†] Peter Hinterdorfer,[†] and Christoph Romanin*[,†]

Institute for Biophysics, University of Linz, Altenbergerstrasse 69, 4020 Linz, Austria, Institute of Biochemistry, Biocenter, Johann Wolfgang Goethe-Universität Frankfurt, Marie Curie Strasse 9, D-60439 Frankfurt, Germany, and Neurobiologie des Canaux Ioniques, INSERM U 464, Institut Fédératif de Recherche Jean Roche, Secteur Nord de la Faculté de Médecine, Boulevard Pierre Dramard, 13 916 Marseille cédex 20, France

Received January 20, 2004. In Final Form: April 26, 2004

Oriented stable binding of functional proteins on surfaces is of fundamental interest for receptor/ligand studies in atomic force microscopy (AFM) and surface plasmon resonance (SPR) experiments. Here we have chosen the His_6-tagged carboxyl-tail (C-tail) of the α_{1C}-subunit of the L-type Ca^{2+} channel and calmodulin (CaM) as its cognitive partner as a model system to develop a new functional surface. Covalently attached self-assembled monolayers on ultraflat gold containing NTA-thiols to which the His_6-tagged C-tail was bound and thiols with triethylene-glycol groups as matrix-thiols represented the system of choice. The topography of this surface was characterized using AFM; its ability to bind C-tail proteins oriented and stable was confirmed by SPR measurements and by complementary force spectroscopy experiments with a CaM_4-construct covalently attached to the tip. The developed anchoring strategy can now be used to study receptor/ligand interactions in general applying force spectroscopy and SPR on His_6-tagged proteins oriented immobilized onto this new NTA-functionalized self-assembled monolayer.

Introduction

Atomic force microscopy (AFM) has become a powerful tool for the investigation of biological systems. Topographic images with high lateral resolution (<10 Å) can be obtained applying very low forces (<10 pN). With the option to operate under physiological conditions, this technique is ideally suited to address important questions in life sciences at the molecular level.[1−7] Force spectroscopy has opened the possibility to detect specific inter- and intramolecular interaction forces at the single-molecule level and to observe molecular recognition of a single receptor−ligand pair. For studying receptor/ligand interactions, ligands are bound to AFM tips and receptors to surfaces (or vice versa). The receptor/ligand complex is formed during tip−surface encounter, and the interaction force is measured when the bond ruptures during tip retraction. Applications include biotin−avidin,[8,9] antibody−antigen,[10−13] sense−antisense DNA,[14,15] and cell recognition proteins.[1,16] Force spectroscopy experiments require stable attachment of the ligands and the receptors to tip and probe surfaces, respectively, with full preservation of the cognitive function of both partners.

A complementary technique to study protein−protein interactions at interfaces is surface plasmon resonance (SPR). SPR provides real-time quantitative and qualitative data on binding interactions between biomolecules.[17,18] A common approach is to bind proteins via His_6-tags to NTA-tagged lipid monolayers, which serve as model cell membranes.[19−21] A macromolecular protease complex (20S Proteasome) has been recently characterized employing NTA lipids.[22,23]

In the present study, we aimed at developing a functional surface, enabling oriented stable immobilization of the His_6-tagged carboxyl-tail (C-tail) of the α_{1C}-

* To whom correspondence should be addressed. E-mail: christoph.romanin@jku.at. Tel: ++43-(0)-732-2468-9274. Fax: ++43-(0)-732-2468-9280.

[†] University of Linz.

[‡] Johann Wolfgang Goethe-Universität Frankfurt.

[§] Institut Fédératif de Recherche Jean Roche.

(1) Dammer, U.; Popescu, O.; Wagner, P.; Anselmetti, D.; Guntherodt, H. J.; Misevic, G. N. *Science* **1995**, *267*, 1173−5.

(2) Florin, E. L.; Moy, V. T.; Gaub, H. E. *Science* **1994**, *264*, 415−7.

(3) Hinterdorfer, P.; Baumgartner, W.; Gruber, H. J.; Schilcher, K.; Schindler, H. *Proc. Natl. Acad. Sci. U.S.A.* **1996**, *93*, 3477−81.

(4) Lee, G. U.; Chrisey, L. A.; Colton, R. J. *Science* **1994**, *266*, 771−3.

(5) Moy, V. T.; Florin, E. L.; Gaub, H. E. *Science* **1994**, *266*, 257−9.

(6) Radmacher, M.; Fritz, M.; Hansma, H. G.; Hansma, P. K. *Science* **1994**, *265*, 1577−9.

(7) Rief, M.; Oesterhelt, F.; Heymann, B.; Gaub, H. E. *Science* **1997**, *275*, 1295−7.

(8) Lee, G. U.; Kidwell, D. A.; Colton, R. J. *Langmuir* **1994**, *10*, 354.

(9) Wong, S. S.; Joselevich, E.; Woolley, A. T.; Cheung, C. L.; Lieber, C. M. *Nature* **1998**, *394*, 52−5.

(10) Allen, S.; Chen, X.; Davies, J.; Davies, M. C.; Dawkes, A. C.; Edwards, J. C.; Roberts, C. J.; Sefton, J.; Tendler, S. J.; Williams, P. M. *Biochemistry* **1997**, *36*, 7457−63.

(11) Hinterdorfer, P.; Schilcher, K.; Baumgartner, W.; Gruber, H. J.; Schindler, H. *Nanobiology* **1998**, *4*, 177−88.

(12) Ros, R.; Schwesinger, F.; Anselmetti, D.; Kubon, M.; Schafer, R.; Pluckthun, A.; Tiefenauer, L. *Proc. Natl. Acad. Sci. U.S.A.* **1998**, *95*, 7402−5.

(13) Willemsen, O. H.; Snel, M. M.; van der Werf, K. O.; de Grooth, B. G.; Greve, J.; Hinterdorfer, P.; Gruber, H. J.; Schindler, H.; van Kooyk, Y.; Figdor, C. G. *Biophys. J.* **1998**, *75*, 2220−8.

(14) Strunz, T.; Oroszlan, K.; Schafer, R.; Guntherodt, H. J. *Proc. Natl. Acad. Sci. U.S.A.* **1999**, *96*, 11277−82.

(15) Boland, T.; Ratner, B. D. *Proc. Natl. Acad. Sci. U.S.A.* **1995**, *92*, 5297−301.

(16) Fritz, J.; Katopodis, A. G.; Kolbinger, F.; Anselmetti, D. *Proc. Natl. Acad. Sci. U.S.A.* **1998**, *95*, 12283−8.

(17) Satoh, A.; Toida, T.; Yoshida, K.; Kojima, K.; Matsumoto, I. *FEBS Lett.* **2000**, *477*, 249−52.

(18) Webster, C. I.; Cooper, M. A.; Packman, L. C.; Williams, D. H.; Gray, J. C. *Nucleic Acids Res.* **2000**, *28*, 1618−24.

(19) Dietrich, C.; Boscheinen, O.; Scharf, K. D.; Schmitt, L.; Tampe, R. *Biochemistry* **1996**, *35*, 1100−5.

(20) Dietrich, C.; Schmitt, L.; Tampe, R. *Proc. Natl. Acad. Sci. U.S.A.* **1995**, *92*, 9014−8.

(21) Radler, U.; Mack, J.; Persike, N.; Jung, G.; Tampe, R. *Biophys. J.* **2000**, *79*, 3144−52.

10.1021/la0498206 CCC: $27.50
Published on Web 05/29/2004

subunit of the L-type Ca^{2+} channel.[24] Voltage-gated L-type Ca^{2+} channels are pore-forming membrane-bound proteins that govern diverse physiological functions, including excitation−contraction coupling in cardiac muscle,[25] hormone secretion,[26] and gene transcription.[27] The activity of L-type Ca^{2+} channels is regulated by Ca^{2+} entry, which induces inactivation of L-type Ca^{2+} channel current as an important negative feedback mechanism.[28] Recent experiments have implicated direct binding of calmodulin (CaM)[29] to the proximal third of the C-tail of the main α_{1C}-subunit of L-type Ca^{2+} channels as a key step in the inactivation mechanism.[30−32] Erickson at al. identified a 73 aa channel segment in the C-tail as the critical preassociation pocket for CaM employing fluorescence resonance energy transfer (FRET) measurements in live cells.[33] In sum, the exact number and role of the different CaM binding sites within the C-tail of the channels remain largely unknown.

To perform single-molecule force spectroscopy experiments between CaM covalently bound to the AFM tip and immobilized His_6-tagged C-tail protein, binding of the C-tail to the surface needs to be stronger than binding of CaM to the C-tail. Moreover, the surface must ensure full preservation of function of immobilized C-tail proteins. Thus, the C-tail/CaM interaction is perfectly suited as a model system to develop a functional surface enabling both orientation and stability of bound His_6-tagged proteins.

Experimental Section

AFM Setup. A Macmode PicoSPM magnetically driven dynamic force microscope (Molecular Imaging, Phoenix, AZ) with a Molecular Imaging Macmode interface was used for AFM measurements. Topography images were recorded using the contact-mode or the mac-mode with MacLevers (Molecular Imaging).

His_6-Tagged C-Tail Proteins. His_6-tagged C-tail protein (amino acids 1490−1704, GenBank accession no. M67515) of the α_1-subunit of the L-type Ca^{2+} channel was expressed and purified using a protocol published recently.[24] A circular dichroism (CD) spectrum of the C-tail protein in buffer solution (1 mg/mL) was recorded (data not shown) on a JASKO CD spectrometer (JASKO Corp., Tokyo, Japan). Thereby detergent (1% Tween) had to be included to keep this protein at this concentration in solution. The spectrum revealed a peak between 210 and 220 nm which is consistent with the presence of α-helices.[34] Furthermore, we have demonstrated functionality of this C-tail protein.[24,35]

NTA- and Matrix-Thiols. The IUPAC names of the substances used in this study (NTA- and matrix-thiol) are [1-carboxy-5-(2-{2-[2-(16-mercapto-hexadecanoyloxy)-ethoxy]-ethoxy}-ethoxy-carbonylamino)-pentyl]-bis-carboxymethylammonium (NTA-thiol) and 16-mercapto-hexadecanoic acid 2-[2-(2-hydroxy-ethoxy)-ethoxy]-ethyl ester (matrix-thiol). Their synthesis and characterization will be described in detail elsewhere (Tinazli, A.; Valiokas, R.; Lata, S.; Picuric, S.; Hutschenreiter, S.; Piehler, J.; Liedberg B.; Tampé, R. Manuscript in preparation). The final products were characterized by NMR and mass spectrometry (MS).

Preparation of SAMs for AFM. For the preparation of thiol-functionalized gold substrates for AFM measurements, flame-annealed (hydrogen gas) gold surfaces (Au(111)) evaporated onto freshly cleaved mica (Molecular Imaging) were incubated in 1 mM solutions of matrix- and NTA-thiol in absolute ethanol for 6−8 h. The thus-prepared SAMs were imaged in water (contact-mode). Formation of the Ni−NTA complex was achieved by incubating the SAM for 5 min in 1 mM NaOH and for 60 min in 40 mM $NiSO_4$. C-Tail proteins were added (10 μg/mL) and after 1 h of incubation time were imaged in a solution containing 150 mM NaCl and 10 mM HEPES (HEPES buffer, pH = 7.4) applying contact-mode.

Statistical Analysis of NTA-Thiol Islands. The statistical analysis of heights of thiol-SAMs was carried out as follows: Five representative AFM images of untreated NTA-thiols were taken and $n = 17$ NTA islands were analyzed using the software PicoScan from Molecular Imaging. Thereby, maximum heights of each profile were taken to calculate the distributions shown in Figure 3c (left). For the C-tail-treated NTA-thiol SAMs, this procedure was repeated ($n = 20$ islands). A single site where C-tail binding was apparently evident at a single island was taken for determination of the right distribution in the figure.

SPR Experiments. Thiol-SAMs for SPR were prepared as follows: SIA Kit Au chips from Biacore (Biacore AB, Uppsala, Sweden) (sonicated for 5 min in absolute ethanol prior to usage) were incubated in 1 mM solutions of either 100 mol % matrix-thiol or 97 mol % matrix- and 3 mol % NTA-thiol in absolute ethanol for 6−8 h. The chips were fixed onto a chip-carrier and transferred to a Biacore X device. All measurements were carried out using HEPES buffer (see above) with 2 mM Ca^{2+} (pH = 7.4) as running- and sample-buffer at a temperature of 25 °C. The flow rate was 30−40 μL/min. The chips were treated for 2 min with 10 mM Ni^{2+} solution before adding C-tail protein (90 μL, 10 μg/mL) and CaM (60 μL, 1 μM).

Force Spectroscopy Measurements. The CaM_4-construct used in all force microscopy studies was generated according to single-step cloning of AvaI contamers[36] using the cDNA of rat calmodulin and subcloned in a custom-made expression vector.[37] The protein containing two cysteins on its C-terminal end was purified using Ni^{2+}-affinity (Novagen, Madison, WI) or phyenyl-sepharose hydrophobic chromatography (Pharmacia, New York, NY), concentrated, and dialyzed into the final buffer (0.1 M Tris, pH = 7.5).[38] Its functionality has been shown in gel-shift assays and in unfolding studies.[38] Before binding to the AFM tip, it was incubated in 20 mM dithiothreitol (DTT) (30 min) to ensure the presence of free SH-groups. The DTT was then removed using spin-columns (Micro Bio-Spin Chromatography Columns, BIO-RAD, Hercules, CA). The synthesis of the poly(ethylene glycol) (PEG) cross-linker (PDP−PEG−NHS), the functionalization of the AFM tip, the binding of the PEG cross-linker to the tip, and the conjugation of the protein were carried out as reviewed.[39] All experiments were done in HEPES buffer with 2 mM Ca^{2+} (pH = 7.4) at a loading rate of 1.8 nN/s. The block was performed with 2 μM CaM. Mathematical analysis of unbinding curves was performed using a self-developed algorithm described in detail from Baumgartner at al.[40,41] For quantification of forces, only unbinding events similar to the one shown in Figure 5a were

(22) Dorn, I. T.; Eschrich, R.; Seemuller, E.; Guckenberger, R.; Tampe, R. *J. Mol. Biol.* **1999**, *288*, 1027−36.
(23) Thess, A.; Hutschenreiter, S.; Hofmann, M.; Tampe, R.; Baumeister, W.; Guckenberger, R. *J. Biol. Chem.* **2002**, *277*, 36321−8.
(24) Mouton, J.; Feltz, A.; Maulet, Y. *J. Biol. Chem.* **2001**, *276*, 22359−67.
(25) Bers, D. M. *Excitation-Contraction Coupling and Cardiac Contractile Force*; Kluwer Academic: Dortrecht, 1991.
(26) Artalejo, C. R.; Adams, M. E.; Fox, A. P. *Nature* **1994**, *367*, 72−6.
(27) Murphy, T. H.; Worley, P. F.; Baraban, J. M. *Neuron* **1991**, *7*, 625−35.
(28) McDonald, T. F.; Pelzer, S.; Trautwein, W.; Pelzer, D. J. *Physiol. Rev.* **1994**, *74*, 365−507.
(29) Chin, D.; Means, A. R. *Trends Cell Biol.* **2000**, *10*, 322−8.
(30) Peterson, B. Z.; DeMaria, C. D.; Adelman, J. P.; Yue, D. T. *Neuron* **1999**, *22*, 549−58.
(31) Romanin, C.; Gamsjaeger, R.; Kahr, H.; Schaufler, D.; Carlson, O.; Abernethy, D. R.; Soldatov, N. M. *FEBS Lett.* **2000**, *487*, 301−6.
(32) Zuhlke, R. D.; Pitt, G. S.; Deisseroth, K.; Tsien, R. W.; Reuter, H. *Nature* **1999**, *399*, 159−62.
(33) Erickson, M. G.; Liang, H.; Mori, M. X.; Yue, D. T. *Neuron* **2003**, *39*, 97−107.
(34) Alder, A. J.; Greenfield, N. J.; Fasman, G. D. *Methods Enzymol.* **1973**, *27*, 675−735.
(35) Mouton, J.; Ronjat, M.; Jona, I.; Villaz, M.; Feltz, A.; Maulet, Y. *FEBS Lett.* **2001**, *505*, 441−4.
(36) Hartley, J. L.; Gregori, T. J. *Gene* **1981**, *13*, 347−53.
(37) Carrion-Vazquez, M.; Oberhauser, A. F.; Fowler, S. B.; Marszalek, P. E.; Broedel, S. E.; Clarke, J.; Fernandez, J. M. *Proc. Natl. Acad. Sci. U.S.A.* **1999**, *96*, 3694−9.
(38) Carrion-Vazquez, M.; Oberhauser, A. F.; Fisher, T. E.; Marszalek, P. E.; Li, H.; Fernandez, J. M. *Prog. Biophys. Mol. Biol.* **2000**, *74*, 63−91.
(39) Riener, C. K.; Kada, G.; Stroh, C. M.; Kienberger, F.; Hinterdorfer, P.; Schindler, H.; Schutz, G.; Schmidt, T.; Hahn, C.; Gruber, H. J. *Recent Res. Dev. Bioconj. Chem.* **2002**, *1*, 133−49.
(40) Baumgartner, W.; Hinterdorfer, P.; Schindler, H. *Ultramicroscopy* **2000**, *82*, 85−95.

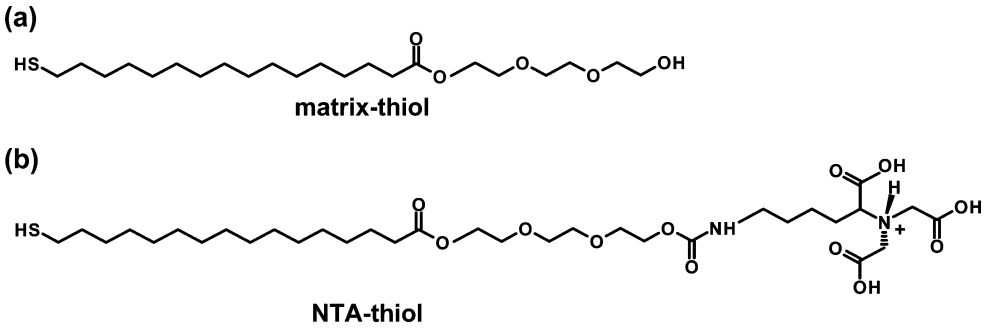

Figure 1. Chemical structures of the matrix-thiol (a) and the NTA-thiol in a fully protonated state (b).

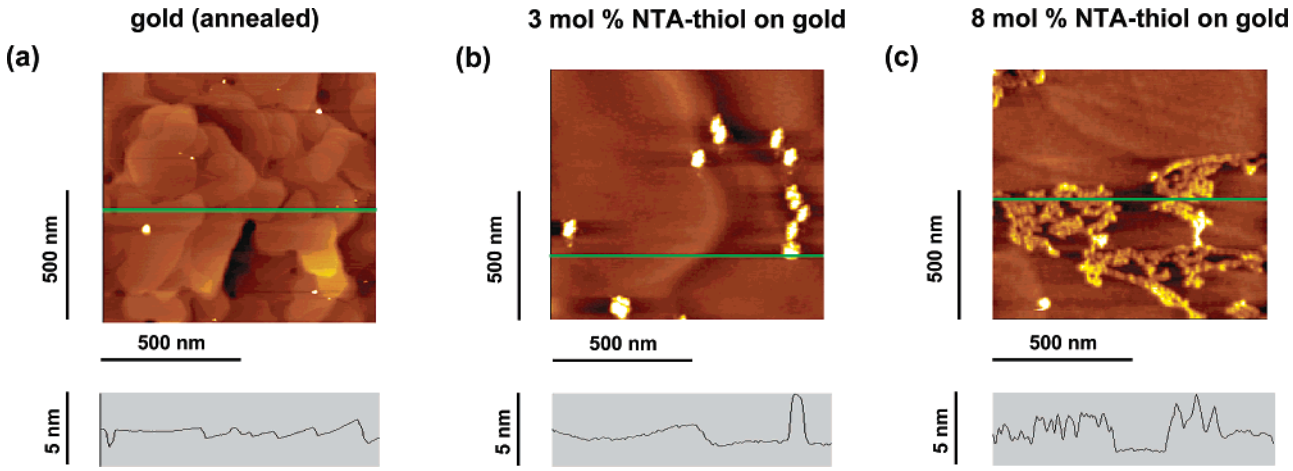

Figure 2. (a) Contact-mode AFM images (top) and corresponding height profiles (bottom) of the flame-annealed ultraflat gold substrate on mica in water. (b,c) AFM images and height profiles of covalently bound SAMs formed from 3 mol % (concentration in solution) NTA-thiol (97 mol % matrix-thiol) (b) and 8 mol % NTA-thiol (92 mol % matrix-thiol) (c) in buffer solution.

taken.[40,41] Unspecific adsorption was generally absent. Multiple jumps-off contacts were observed in ~1% of all force−distance cycles in both the experiment without and with free CaM (blocking experiment) but were eliminated during the selection process. All calculations were done using the software Matlab 6.1 (The MathWorks Inc., Natick, MA).

Results and Discussion

The novel surface that was developed consists of thiols with triethylene-glycol units (Figure 1a) that are known to prevent nonspecific binding of proteins[42−45] and homologous thiols functionalized with terminal NTA headgroups (Figure 1b). Similar thiols with identical NTA headgroups have already been successfully used with liquid crystals[46] and His_6-tagged proteins.[47] A self-assembled monolayer (SAM) with an intermediate density of NTA/Ni^{2+} functions covalently bound to ultraflat gold is formed from these thiols.

Topography of SAMs. Figure 2a shows contact-mode AFM images in water of gold surfaces, which were flame-annealed with hydrogen gas prior use. Characteristic "terrace" structures with a height of about 1−2 nm (height profile) were clearly resolved. Figure 2b depicts SAMs on these gold surfaces formed from an ethanolic solution containing 3 mol % NTA-thiol and 97 mol % matrix-thiol (total thiol concentration, 1 mM). This surface lacks the terrace structures observed on untreated gold, indicating complete coverage with SAMs. The NTA-thiols seemed to agglomerate under these experimental conditions, forming "islands", the extension of which increased with increasing NTA-thiol concentrations in solution (Figure 2c). Height profiles showed a maximum relative height for NTA-thiol islands of about 2.5 nm (see below and Figure 3c).

C-Tail Protein Binding Visualized by AFM. To enable binding of the His_6-tagged C-tail protein, SAMs were treated with NaOH and Ni^{2+} before adding the protein. Figure 3 shows high-resolution AFM images of thiol-SAMs obtained in the absence (Figure 3a) and presence (Figure 3b) of the C-tail protein. The NTA sites at which protein binding occurred are marked with arrows in Figure 3b. Due to an apparent accumulation of C-tail protein on the NTA islands, single molecules could not be clearly resolved. Binding is also evident from the comparison of height profiles as depicted in the lower panels of Figure 3a,b. Furthermore, a statistical height analysis from respective AFM images of NTA islands without (Figure 3a) and with (Figure 3b) C-tail protein was performed (Figure 3c). The height of the NTA-thiols relative to the surrounding matrix-thiols revealed an average value of 2.5 (±0.1) nm (n = 17). This value is consistent with that obtained by Thomson et al.[48] where slightly different thiols with identical terminal groups were used. The difference between theoretically expected values of the length difference between matrix- and NTA-

(41) Kienberger, F.; Kada, G.; Gruber, H. J.; Pastushenko, V. P.; Riener, C. K.; Trieb, M.; Knaus, H.-G.; Schindler, H.; Hinterdorfer, P. *Single Mol.* **2000**, *1*, 59−65.
(42) Mrksich, M.; Chen, C. S.; Xia, Y.; Dike, L. E.; Ingber, D. E.; Whitesides, G. M. *Proc. Natl. Acad. Sci. U.S.A.* **1996**, *93*, 10775−8.
(43) Mrksich, M.; Whitesides, G. M. *Annu. Rev. Biophys. Biomol. Struct.* **1996**, *25*, 55−78.
(44) Pale-Grosdemange, C.; Simon, E. S.; Prime, K. L.; Whitesides, G. M. *J. Am. Chem. Soc.* **1991**, *113*, 12−20.
(45) Schmitt, L.; Ludwig, M.; Gaub, H. E.; Tampe, R. *Biophys. J.* **2000**, *78*, 3275−85.
(46) Luk, Y. Y.; Tingey, M. L.; Hall, D. J.; Israel, B. A.; Murphy, C. J.; Bertics, P. J.; Abbott, N. L. *Langmuir* **2003**, *19*, 1671−80.
(47) Sigal, G. B.; Bamdad, C.; Barberis, A.; Strominger, J.; Whitesides, G. M. *Anal. Chem.* **1996**, *68*, 490−7.
(48) Thomson, N. H.; Smith, B. L.; Almqvist, N.; Schmitt, L.; Kashlev, M.; Kool, E. T.; Hansma, P. K. *Biophys. J.* **1999**, *76*, 1024−33.

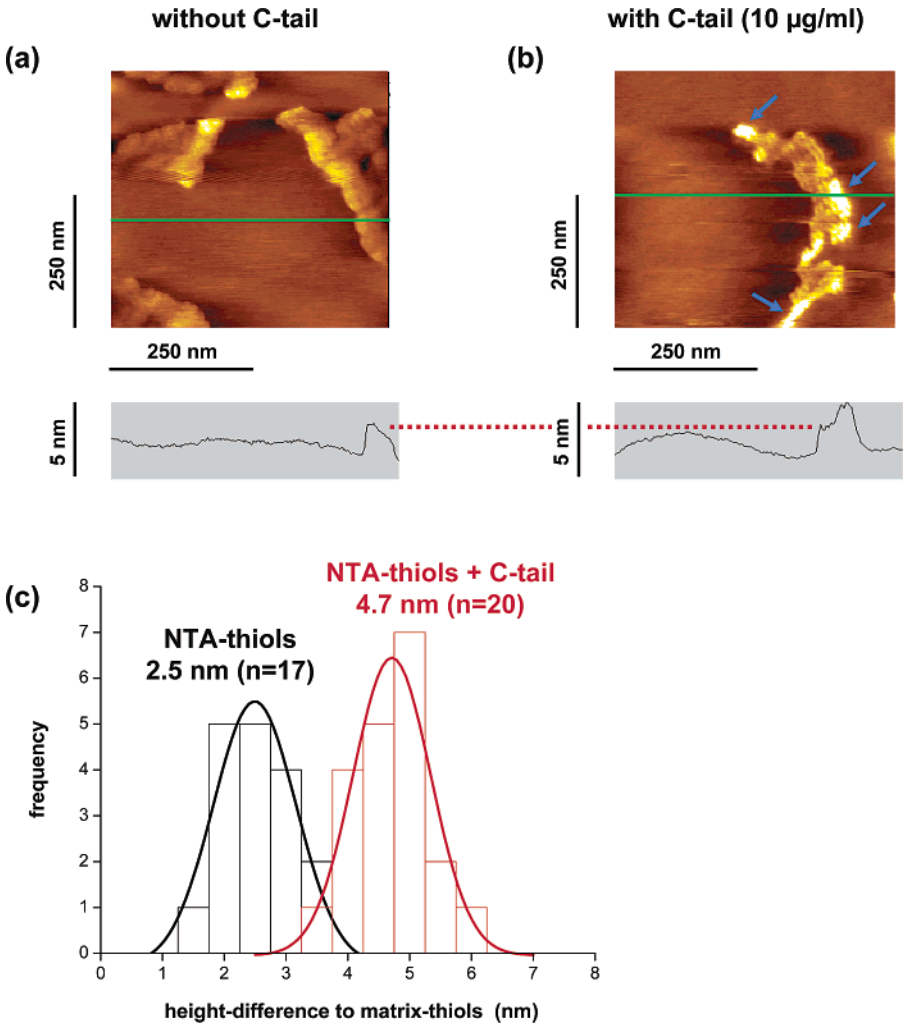

Figure 3. (a,b) Images and corresponding height profiles of SAMs formed from ethanolic solutions containing 8 mol % NTA-thiol (92 mol % matrix-thiol) without (a) and with (b) C-tail protein (10 μg/mL, 60 min incubation of Ni^{2+}-preloaded SAM) in HEPES buffer. The blue arrows indicate NTA-thiols with C-tail protein bound; the red dotted line indicates the height differences between panels a and b. **(**c**)** Statistical analysis (five representative AFM images, see the Experimental Section) of heights of NTA-thiols with and without bound C-tail protein relative to surrounding matrix-thiols.

thiol molecules and the height difference within the SAM can be explained by the distinct arrangement of the thiols: The alkyl chains of the matrix-thiols tilt from the surface normal by around 30° as observed by IR spectroscopy and X-ray diffraction.[49,50] In contrast, the longer NTA-thiols most likely adopt an orientation perpendicular to the surface due to the bulky NTA groups and their tendency to self-aggregate. Statistical analysis of relative heights of the C-tail protein treated NTA-thiols revealed a significantly ($p < 0.001$) higher average value of 4.7 ($\pm$0.1) nm ($n = 20$) (Figure 3c), indicating C-tail binding to this surface.

SPR-Confirmed Oriented C-Tail Protein Binding. To examine whether in this system the C-tail proteins were bound in proper orientation that allows for interaction with CaM, SPR measurements were carried out on Biacore gold chips coated with the same type of SAMs (3 mol % NTA-thiol and 97 mol % matrix-thiol in ethanolic solution, activated with Ni^{2+}). The results are summarized in Figure 4. Binding of the His_6-tagged C-tail protein was clearly dependent on the presence of the NTA-thiols (Figure 4a). For semiquantitative analysis of the binding specificity, RU values reached at the end of the C-tail protein injection (90 μL) were compared between NTA-functionalized chips and control chips with matrix-thiols (Figure 4c). Specific adsorption of the protein was significantly higher than the nonspecific binding onto the matrix-thiols (18.4% $\pm$ 1.1% relative to specific binding; $n = 4$). Additional experiments (data not shown) performed in the presence of 200 mM imidazol on the same NTA-functionalized gold chips revealed no binding of C-tail protein. This confirmed specific binding via NTA/His_6 since a concentration of 200 mM imidazol is known to efficiently block the NTA groups.[41] When CaM was added at a concentration of 1000 nM, known to be sufficient (well above the K_D) for the binding,[24] specific binding to the C-tail protein was observed (Figure 4b), which indicates proper orientation of the C-tail/CaM-binding domain. Nonspecific adsorption of CaM in the absence of the C-tail protein was significantly smaller (27.1% $\pm$ 1.7%; $n = 3$; Figure 4d). Binding specificities were calculated analogously as described above for RU values reached at the end of the CaM injection (60 μL).

Force Microscopy Studies on the Single-Molecule Level. Based on these results obtained by SPR, force spectroscopy experiments were performed to directly measure interaction forces between the C-tail protein and CaM. For this, C-tail proteins were bound to gold

(49) Feldman, K.; Haehner, G.; Spencer, N. D.; Harder, P.; Grunze, M. *J. Am. Chem. Soc.* **1999**, *121*, 10134−10141.
(50) Harder, P.; Grunze, M.; Dahint, R.; Whitesides, G. M.; Laibinis, P. E. *J. Phys. Chem. B* **1998**, *102*, 426−36.

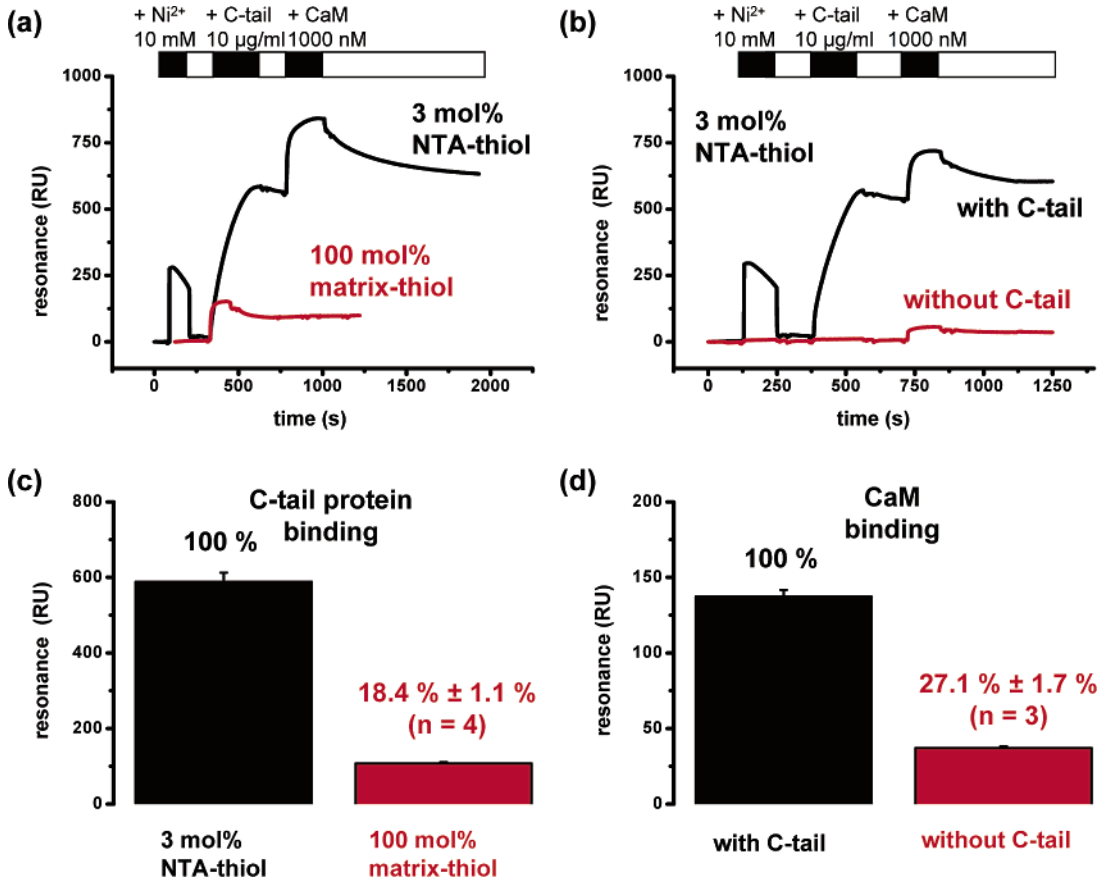

Figure 4. (a) Representative SPR sensorgrams of Biacore gold chips coated with SAMs from ethanolic solutions containing 3 mol % NTA-thiol (97 mol % matrix-thiol) (black line) and 100 mol % matrix-thiol (red line) as a control. The C-tail protein (90 μL, 10 μg/mL) was added following preloading of SAMs with Ni^{2+}. (b) Representative SPR sensorgrams of a Biacore gold chip coated with SAMs from ethanolic solutions containing 3 mol % NTA-thiol (97 mol % matrix-thiol) without (red line) and with (black line) C-tail protein (90 μL, 10 μg/mL) immobilized. CaM (60 μL, 1000 nM) was then added to evaluate the binding ability of the C-tail protein. (c) Semiquantitative analysis of binding specificity: RU values at the end of the C-tail injection (90 μL) were determined from the sensorgrams, and a ratio between the values obtained on the NTA-functionalized chip (black curve) and those obtained on the chip covered with matrix-thiols (red curve) was calculated. (d) Binding specificity calculated as described in panel c for the CaM injection (60 μL).

substrates as described in this study (Figure 3b) and a CaM_4-construct was covalently attached to the AFM tip. The tip surface chemistry used[3,11,39,41,51−55] renders, due to its low surface density of ligands on the tips, single-molecule experiments possible. In addition, ligands can freely diffuse about the tip because they are coupled via a flexible, 6 nm long tether (heterobifunctional poly(ethylene glycol) derivative) and thus enable unconstrained recognition. Forces required to dissociate single C-tail/CaM_4 bonds ("unbinding force") were measured in force−distance cycles (Figure 5). In the horizontal region during tip/surface approach (trace, curve 1, red line), there is no measurable interaction between tip and surface because the tip is too far from the surface. The linear region (curve 2) in both trace and retrace (tip retraction) reflects direct tip/surface contact, which leads to a linear change in the detection angle of the cantilever in dependence of the *z*-position of the cantilever. In the region of the initial tip/sample contact (curve 3), the signal slightly deviates from linearity, which is explained by the presence of the soft thiol-SAM and the proteins on the substrate. In the case of C-tail protein/CaM_4 binding, a recognition signal appears upon tip retraction (Figure 5a, retrace, curve 4), caused by the physical connection between the CaM_4 molecule on the tip and the C-tail protein on the surface. Its nonlinear shape is determined by the elastic properties of the tether by which the CaM_4-contruct is coupled to the AFM tip.[11,54] The force applied to the C-tail/CaM_4 bond increases during further tip/surface retraction until the bond ruptures at a characteristic unbinding force (here 120−130 pN) and the cantilever flips back into the resting position (Figure 5a). A recognition signal as observed in Figure 5a was present in 80 of about 800 force−distance cycles recorded (binding probability of 10%). Specific selection of the force−distance cycles with unbinding events was performed as described in the Experimental Section.[40] Considering the low density of NTA-thiol-bound C-tail proteins on the surface and the lateral drift of the AFM tip, this value is comparable with values obtained in similar studies in our lab.[11,53] Force spectroscopy performed on surfaces covered with less than 8 mol % NTA-thiols would result in lower binding probabilities and was therefore not carried out. The disruption of CaM_4 occurred over a stretch of about 80 nm, most probably because of the stretching of the involved molecules (C-tail

(51) Hinterdorfer, P.; Gruber, H. J.; Kienberger, F.; Kada, G.; Riener, C. K.; Borken, C.; Schindler, H. *Colloids Surf.* **2002**, *23*, 115−23.
(52) Hinterdorfer, P.; Kienberger, F.; Raab, A.; Gruber, H. J.; Baumgartner, W.; Kada, G.; Riener, C. K.; Wielert-Badt, S.; Borken, C.; Schindler, H. *Single Mol.* **2000**, *1*, 99−103.
(53) Kada, G.; Blayney, L.; Jeyakumar, L. H.; Kienberger, F.; Pastushenko, V. P.; Fleischer, S.; Schindler, H.; Lai, F. A.; Hinterdorfer, P. *Ultramicroscopy* **2001**, *86*, 129−37.
(54) Raab, A.; Han, W.; Badt, D.; Smith-Gill, S. J.; Lindsay, S. M.; Schindler, H.; Hinterdorfer, P. *Nat. Biotechnol.* **1999**, *17*, 901−5.
(55) Riener, C. K.; Stroh, C. M.; Ebner, A.; Klampfl, C.; Gall, A.; Romanin, C.; Lyubchenko, Y. L.; Hinterdorfer, P.; Gruber, H. J. *Anal. Chim. Acta* **2003**, *479*, 59−75.

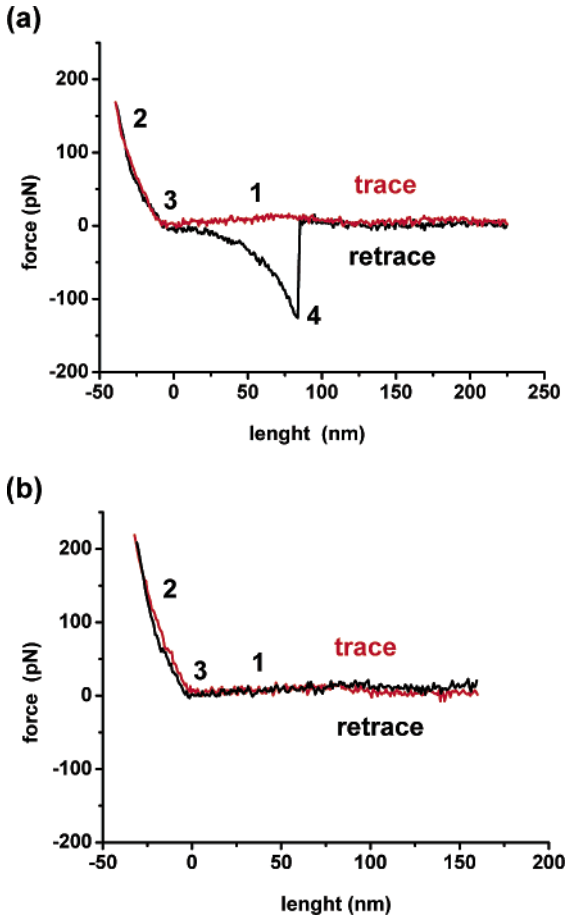

Figure 5. (a) Representative force−distance cycle showing the interaction between NTA-thiol-bound C-tail protein and a CaM_4-construct covalently attached to the AFM tip. The recognition signal in the retrace corresponds to a single-molecule binding event. (b) Control experiment in which an excess of free CaM (2 μM) was added to the solution to block binding. Note that the recognition signal in the retrace disappeared.

protein, cross-linker, CaM_4-construct).[38] When CaM was added into the solution, recognition disappeared (Figure 5b) in almost all force−distance cycles. Apparently, the binding sites for CaM of the C-tail protein on the surface were blocked by CaM, thereby preventing recognition by CaM molecules on the tip. The remaining binding probability of 1% is attributed to a less than 100% efficiency of the block and/or to rarely occurring nonspecific tip−probe adhesion. These results confirm that the recognition events observed and the unbinding forces measured indeed arise from specific C-tail/CaM_4 interactions. An empirical probability-density function was calculated from all force−distance cycles containing a recognition signal and normalized to unity area (Figure 6, solid line). The dotted line in Figure 6 represents the control (block) experiment. It was normalized to an area corresponding to the decrease of the binding probability from 10% to 1% (1/10). From this probability-density function, an average unbinding force of 130 pN was calculated. This high value probably results from the existence of two different binding sites for one molecule of CaM within the C-tail. This finding supports the proposed Ca^{2+}-dependent switching mechanism where at high Ca^{2+} concentrations both binding sites are concomitantly occupied.[33]

Summary and Conclusions

The C-tail of the α_1-subunit of the L-type Ca^{2+} channel and its interaction partner in the Ca^{2+}-induced inactivation process in living cells, CaM, were chosen in this study to develop a functional surface achieving the oriented binding of His_6-tagged proteins. Since the C-tail protein possesses a His_6-tag on the N-terminal side, its binding via NTA/His_6 onto NTA-labeled molecules enables an appropriate approach. The strong interaction force of 150−200 pN measured for the NTA/His_6 interaction[41] makes this anchoring strategy even more suitable particularly for force spectroscopy. A new system using ultraflat gold and covalently bound antiadsorptive thiols as matrix-thiols as well as NTA-functionalized thiols was introduced. Binding of the C-tail protein onto the NTA-thiols of this surface did not disturb the CaM binding capability as shown in SPR experiments. The surface was characterized using AFM, and the specific binding of the protein onto the NTA-thiols was visualized applying the AFM contact-mode. Force spectroscopy was performed with CaM_4 attached to the AFM tip via a flexible cross-linker. This was the first time that direct single-molecule interaction forces between the C-tail and CaM were measured. More than 800 force−distance cycles were carried out in a row which demonstrated the stability of the NTA/His_6 bond. Control experiments, in which CaM was added to the solution to block bound C-tail proteins, confirmed unambiguously the specific interaction between the C-tail and CaM. Apparently this surface allows for covalent attachment of NTA-thiols while preserving the functionality of the stable bound His_6-tagged proteins. Therefore it provides a convenient system for the examination of the interaction between these two physiologically important molecules. Moreover, this NTA-functionalized SAM might serve as a general system to characterize His_6-tagged proteins by force spectroscopy and SPR where other commonly used substrates such as for example mica or phospholipid bilayers are not appropriate surfaces.

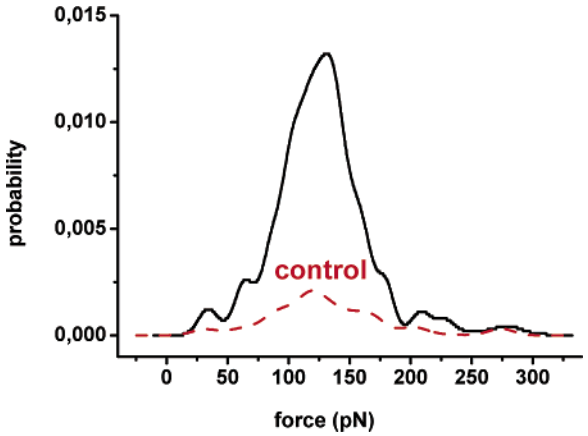

Figure 6. Empirical probability-density functions of C-tail protein/CaM_4 interactions (black, solid line) calculated from unbinding forces obtained in force−distance cycles at a loading rate of 1.8 nN/s. The binding probability decreased dramatically when free CaM was present in solution (control; red, dotted line).

Acknowledgment. The authors thank Dr. Mariano Carrion-Vazquez for providing us with the CaM_4-construct used in force spectroscopy experiments and Dr. Rita Grandori and Maria Šamalikova for helping us with the CD-measurements. This work was supported by the Austrian Academy of Sciences (DOC 13/2001), the Austrian Science Fund (P-15387, P-15295, P-14549), and the Austrian National Bank (NB 10352).

LA0498206